INFECTION AND IMMUNITY, Aug. 2002, p. 4204–4214 Vol. 70, No. 8
0019-9567/02/$04.00+0 DOI: 10.1128/IAI.70.8.4204–4214.2002

Yersiniabactin Production Requires the Thioesterase Domain of HMWP2 and YbtD, a Putative Phosphopantetheinylate Transferase

Alexander G. Bobrov, Valerie A. Geoffroy,† and Robert D. Perry*

Department of Microbiology, Immunology, and Molecular Genetics, University of Kentucky, Lexington, Kentucky

Received 31 January 2002/Returned for modification 15 March 2002/Accepted 2 May 2002

One requirement for the pathogenesis of *Yersinia pestis*, the causative agent of bubonic plague, is the yersiniabactin (Ybt) siderophore-dependent iron transport system that is encoded within a high-pathogenicity island (HPI) within the *pgm* locus of the *Y. pestis* chromosome. Nine gene products within the HPI have demonstrated functions in the nonribosomal peptide synthesis (NRPS)/polyketide (PK) synthesis or transport of Ybt. NRPS/PK synthetase or synthase enzymes are generally activated by phosphopantetheinylation. However, no products with similarities to known phosphopantetheinyl (P-pant) transferases were found within the *pgm* locus. We have identified a gene, *ybtD*, encoded outside the HPI and *pgm* locus, that is necessary for function of the Ybt system and has similarities to other P-pant transferases such as EntD of *Escherichia coli*. A deletion within *ybtD* yielded a strain (KIM6-2085+) defective in siderophore production. This strain was unable to grow on iron-deficient media at 37°C but could be cross-fed by culture supernatants from Ybt-producing strains of *Y. pestis*. The promoter region of *ybtD* was fused to *lacZ*; β-galactosidase expression from this reporter was not regulated by the iron status of the bacterial cells or by YbtA, a positive regulator of other genes of the *ybt* system. The *ybtD* mutant failed to express indicator Ybt proteins (high-molecular-weight protein 1 [HMWP1], HMWP2, and Psn), a pattern similar to those seen with several other *ybt* biosynthetic mutants. In contrast, cells containing a single amino acid substitution (S2908A) in the terminal thioesterase domain of HMWP2 failed to exhibit any *ybt* regulatory defects but did not elaborate extracellular Ybt under iron-deficient conditions.

To cause infections nearly all pathogenic bacteria must remove iron, an essential trace nutrient, from host iron- and/or heme-chelating proteins (14, 50, 75). *Yersinia pestis*, the causative agent of bubonic and pneumonic plague, possesses an ABC hemoprotein transport system (Hmu) that allows it to use a variety of host hemoproteins as a source of iron (40, 73) as well as a Has/hemophore system that may not be functional (62). Analysis of the sequence of CO92 (*Y. pestis* biotype *orientalis*) (53) and KIM10+ (*Y. pestis* biotype *mediaevalis*) (21) revealed nine potentially functional inorganic iron transport systems; three of these have demonstrated iron acquisition ability. The Yfu system (35) belongs to a family of ABC iron transporters present in *Yersinia enterocolitica* (Yfu), neisseriae (Fbp), *Haemophilus influenzae* (Hit), *Actinobacillus pleuropneumoniae* (Afu), and *Serratia marcescens* (Sfu) (8). The *Y. pestis* Yfe system belongs to a family of cation-transporting ABC systems and transports both iron and manganese. This system acquires iron during the later stages of plague (5, 6).

The yersiniabactin (Ybt) iron transport system produces a siderophore composed of phenolate, thiazoline, and thiazolidine rings (16, 22, 55) via a nonribosomal peptide synthesis (NRPS)/polyketide (PK) synthesis scheme. The Ybt siderophore has considerable similarity to the siderophores pyochelin and anguibactin, produced by *Pseudomonas aeruginosa* and *Vibrio anguillarum*, respectively (20, 42). The Ybt iron acquisition system is essential for the virulence of *Y. pestis* during the early stages of infection in mice (5) and appears to be the primary iron acquisition system of plague (56). Ybt biosynthetic, regulatory, and transport genes are encoded within a high-pathogenicity island (HPI) that is present in highly pathogenic isolates of *Y. pestis*, *Yersinia pseudotuberculosis*, and *Y. enterocolitica*, as well as several types of pathogenic *Escherichia coli* (10, 11, 15, 30, 38, 60, 66). In *Y. pestis*, the HPI resides within the *pgm* locus, a 102-kb region of chromosomal DNA subject to high-frequency deletion (11, 12, 27, 30, 37, 48).

Iron from Fe-Ybt is transported into the cell via a TonB-dependent OM receptor (termed Psn in *Y. pestis* and FyuA in *Y. enterocolitica*) in conjunction with an ABC transport system encoded by *ybtP* and *ybtQ*. Psn also binds the bacteriocin pesticin (24–26, 39, 45, 61). Both YbtP and YbtQ are necessary for use of iron from Ybt and resemble inner membrane permeases fused to an ATP-binding domain. No periplasmic-binding protein has been identified for the Ybt system (9, 24, 30). YbtA is a transcriptional regulator of the AraC family that activates transcription of *ybt* biosynthetic and transport operons and represses transcription from its own promoter (23).

Ybt biogenesis uses a mixed NRPS/PK synthesis mechanism that assembles the siderophore from salicylate, a linker group derived from malonyl coenzyme A, three molecules of cysteine, and three methyl groups donated by *S*-adenosylmethionine (30). The requirement of six gene products (high-molecular-weight protein 1 [HMWP1], HMWP2, YbtE, YbtS, YbtT, and YbtU) for in vivo Ybt synthesis has been clearly demonstrated. YbtS likely participates in salicylate biosynthesis (4, 30). YbtE adenylates salicylate and transfers this activated compound to HMWP2 (31). HMWP2, encoded by *irp2*,

* Corresponding author. Mailing address: Department of Microbiology, Immunology, and Molecular Genetics, MS415 Medical Center, University of Kentucky, Lexington, KY 40536-0084. Phone: (859) 323-6341. Fax (859) 257-8994. E-mail: rperry@pop.uky.edu.

† Present address: Laboratoire de Microbiologie et de Génétique, CNRS, UPRES-A7010, Université Louis-Pasteur, 67000 Strasbourg, France.

possesses NRPS domains involved in the initial cyclization and condensation reactions involving salicylate and two cysteine molecules (30, 31, 36, 71). YbtU reduces the middle thiazoline ring to a thizolidine structure (51). HMWP1, encoded by *irp1*, contains PK/fatty acid synthase and modified NRPS domains that add the branched isobutyryl-alcohol linker and the last thiazoline moiety. YbtT contains a thioesterase (TE) domain (4, 30) and may be involved in removing aberrant structures from the enzymatic complex, while the terminal TE domain of HMWP1 is hypothesized to remove the completed siderophore from the enzyme complex (33).

NRPS/PK synthetase or synthase enzymes are generally activated by phosphopantetheinylation. Phosphopantetheinyl (P-pant) transferases transfer the 4′-phosphopantetheine moiety of coenzyme A to a specific site on the NRPS and PK enzymes. Activated acyl groups or amino acids are subsequently added to these tethers in preparation for the assembly of the compounds. Phosphopantetheinylation of a peptidyl carrier protein domain of HMWP1 (PCP3) has been demonstrated in vitro using *E. coli* EntD (30). No gene encoding an apparent P-pant transferase is present within the HPI or the *pgm* locus. Here we report on genes involved in the first and last steps of Ybt biogenesis—activation of the NRPS/PK synthetase complex by phosphopantetheinylation and cleavage of the completed siderophore by the terminal TE domain of HMWP1.

MATERIALS AND METHODS

Bacterial strains, media, and culture conditions. All relevant characteristics of strains used in this study are presented in Table 1. All the *Y. pestis* strains used in this study were derived from KIM6+, an avirulent strain that possesses all of the known *Y. pestis* virulence determinants except for pCD1, a 70.5-kb plasmid encoding the low-calcium response (Lcr) regulon. (27, 68) The Lcr virulence regulon is unrelated to the Pgm^+ phenotype and has no demonstrable role in iron metabolism (57, 59).

All strains were stored at −20°C in phosphate-buffered glycerol. *Y. pestis* cells were grown routinely at 30°C on Congo red (72) from glycerol stocks and then grown in heart infusion broth (Difco Laboratories) or on tryptose-blood agar base (Difco). For iron-deficient growth, *Y. pestis* cells were grown in the chemically defined medium PMH or PMH2 (33) which had been extracted prior to use with Chelex 100 resin (Bio-Rad Laboratories) (70). Growth of the cultures was monitored by determining the optical density at 620 nm with a Genesys5 spectrophotometer (Spectronic Instruments, Inc.). Residual iron not removed from deferrated PMH or PMH2 by the resin can be precipitated by the addition of 0.5 mM $NaCO_3$, 0.01 mM $MnCl_2$, and 4.0 mM $CaCl_2$ (PMH-S and PMH2-S) or chelated by supplementation with 2,2′-dipyridyl (PMH-DIP) at a concentration of 100 μM. PMH-S, PMH2-S, and PMH-DIP plates were solidified with 1% agarose. PMH-S, PMH2-S, and/or PMH-DIP plates were subsequently used in cross-feeding experiments or to determine the growth characteristics of the *ybt* mutants at 37°C as previously described (25). For iron-replete growth, *Y. pestis* strains were cultivated in PMH2 supplemented with 10 μM $FeCl_3$.

All glassware used for iron-restricted studies was soaked overnight in chromic-sulfuric acid (46.3 g of $K_2Cr_2O_7$ per liter of 11.25 M sulfuric acid) or ScotClean (OWL Scientific, Inc) to remove contaminating iron and copiously rinsed in deionized water. *E. coli* cells were grown on Luria broth. Where appropriate, ampicillin (100 μg/ml), spectinomycin (100 μg/ml), tetracycline (6.25 μg/ml), streptomycin (50 μg/ml), kanamycin (50 μg/ml), or chloramphenicol (30 μg/ml) was added to cultures.

Plasmids, sequencing, and recombinant DNA techniques. All the plasmids used in this study are listed in Table 1. Plasmids were purified from overnight cultures by alkaline lysis (7) and further purified when necessary by polyethylene glycol precipitation (41). Standard cloning and recombinant DNA methods (63) were used to construct the various plasmids in Table 1. A standard $CaCl_2$ procedure was used to introduce plasmids into *E. coli* (63). *Y. pestis* cells were transformed by electroporation as previously described (25). Plasmid DNA and PCR products were sequenced by either Retrogen, Inc., or in our laboratory. Sequencing reactions in our laboratory were performed via the dideoxynucleotide chain termination method (64) using ^{35}S-dATP (Amersham/USB), Sequenase (version 2.0; Amersham/USB), and 7-deaza-dGTP (Boehringer Mannheim Biochemicals). Samples were electrophoresed through a 6% polyacrylamide gel containing 8.3 M urea (Sigma) cast in Tris-borate-EDTA buffer (63). Dried gels were exposed at room temperature to Kodak Biomax MR film. Synthetic oligonucleotide primers were purchased from Integrated DNA Technologies.

Nucleotide sequence accession number. The *ybtD* sequence may be found using GenBank accession number AE009952, which contains the entire *Yersinia pestis* KIM10+ genome sequence (21). BLAST searches of the *Yersinia pestis* KIM10+ genome may be performed at the Web site (http://magpie.genome.wisc.edu/cgi-bin/Authenticate.cgi/uwgp blast.html) for the Genome Center of Wisconsin. KIM10+ is a derivative of KIM6+ lacking plasmid pPCP1 (58)

Generating *ybtD* and *irp2TE* mutant strains. All *Y. pestis* mutant strains were generated by homologous recombination using mutated DNA fragments cloned into suicide vectors carrying the *sacB* gene and an R6K origin of replication. For construction of a Δ*ybtD* strain (KIM6-2085+), a 4.44-kb *Xho*I/*Bgl*II fragment of *Y. pestis* KIM6+ genomic DNA was cloned into *Xho*I/*Bam*HI sites of pWSK29. Isolates containing recombinant plasmids were screened by PCR using *Taq* polymerase with primers ENTD1 (5′-GCCAAGTGTGATTTTGAGGTGA-3′) and ENTD2 (5′-ACGCACGTTGGTTATTATGGCT-3′). Reaction mixtures contained 0.2 mM deoxynucleoside triphosphates and 0.2 μM primers. Reactions consisted of 4 min at 94°C followed by 25 cycles of 20s s at 94°C, 30 s at 55°C, and 30 s at 72°C and a single cycle at 72°C for 7 min. One clone containing the desired insert was designated pYBTD1. A deletion encompassing most of the *ybtD* gene was made by removal of a 774-bp *Eco*RV/*Asu*II fragment from pYBTD1 to yield pYBTD2 (see Fig. 2). A 3.7-kb *Xba*I/*Apa*I fragment from pYBTD2 was cloned into the *Xba*I/*Apa*I sites of the suicide vector pKNG101 creating pYBTD3. The recombinant suicide plasmid was introduced into *Y. pestis* KIM6+ by electroporation. *Y. pestis* isolates with the plasmid recombined into the chromosome were selected on tryptose-blood agar base plates containing 50 μg of streptomycin/ml. As previously described, cells grown overnight without antibiotics were used to select sucrose-resistant isolates that had completed allelic exchange (5). Isolates containing the chromosomal Δ*ybtD* mutation were identified by PCR using *Taq* polymerase with primers ENTD1 (see above) and ENTD3 (5′-CGATTGGCTA GAGAAAGCAGGA-3′). Reaction mixtures contained 0.2 mM deoxynucleoside triphosphates and 0.2 μM primers. Reactions consisted of 3 min at 94°C followed by 25 cycles of 15s s at 94°C, 30 s at 55°C, and 90 s at 72°C and a single cycle at 72°C for 7 min. One isolate, strain KIM6-2085+ (Table 1), was selected for further characterization.

For *trans* complementation of the Δ*ybtD* mutation, a 0.93-kb PCR product was amplified from pYBTD1 using ProofStart *Taq* polymerase (Qiagen) with primers ENTDC-1 (5′-CGCGGATCCTCCTCCAGTCCACAACC-3′) and ENTDC-2 (5′-GCTCTAGACTTCTTTCATATTCAGCCC-3′). Reaction mixtures contained 0.2 mM deoxynucleoside triphosphates and 0.2 μM primers. Reactions consisted of 3 min at 94°C followed by 25 cycles of 20 s at 94°C, 30 s at 55°C, and 90 s at 72°C and a single cycle at 72°C for 7 min. Following digestion with *Bam*HI and *Xba*I, the product was ligated into the *Bam*HI/*Xba*I of pACYC184 generating pYBTD4.

pET22b-HMWP1-TEmut (Table 1) was used to construct an HMWP1-TE^- mutant (KIM6-2086). This plasmid contains a 9,491-bp *Nco*I/*Xho*I fragment from *irp1* in which a single base pair replacement results in the substitution of alanine for serine in the TE domain of HMWP1 at residue 2908. A 1,372-bp *Pvu*II/*Xho*I fragment of pET22b-HMWP1-TEmut was subcloned into the *Sma*I/*Sal*I sites of the suicide plasmid pKNG101, generating pIrp1TE1. The mutation was introduced into *Y. pestis* KIM6+ by allelic exchange as described previously (5). Individual colonies were analyzed for the ability to grow at 37°C in iron-depleted PMH-DIP. One of the isolates that was unable to grow after 24 to 48 h of incubation was analyzed for incorporation of the *irp1* mutation. The *irp1*-TE region of this putative mutant was amplified by PCR using primers TE-PCR1 (5′-CTGTTCAGCCATTCGACG-3′) and TE-PCR2 (5′-AGATGCGCGATGT TGTCG-3′). Reactions consisted of 5 min at 94°C followed by 35 cycles for 30 s at 94°C, 30 s at 50°C, and 30 s at 72°C and a single cycle at 72°C for 7 min. The predicted 595-bp product was purified using a G100-120 Sephadex column. The mutation was confirmed by sequencing the PCR product using primers TE-Seq1 (5′-GTATGTCGGGTGCATCCG-3′) and TE-Seq2 (5′-CTCGCCTTTGGCGT ACAG-3′). For complementation of the *irp1-2086* mutation, this chromosomal mutation was replaced by wild-type *irp1* sequences. A 1,703-bp PCR product from the cloned *irp1* gene (spanning the TE regions) in pPSN3 was amplified using primers YTE-*Xba*I-1 (5′-GCTCTAGAGACGGAGCGAAACAGCGTAT TCC-3′) and TE-*Bam*HI-2 (5′-CGGGATCCGGATGCTCCTGAATGACGTG TACG-3′). Reactions consisted of 4 min at 94°C followed by 30 cycles for 20 s at 94°C, 30 s at 67°C, and 120 s at 72°C and a single cycle at 72°C for 7 min. After digestion with *Bam*HI and *Xba*I, the PCR fragment was ligated into the *Bam*HI/

TABLE 1. Bacterial strains and plasmids used in this study[a]

Strain or plasmid	Relevant characteristic(s)	Reference or Source
E. coli		
DH5α	Cloning host	2
DH5α (λpir)	Strain for propagating plasmids with R6K origins, derived from DH5α	S. C. Straley
Y. pestis		
KIM6+	Pgm^+ (Hms^+ Ybt^+) Lcr^-	25
KIM6	Pgm^- (Δ*pgm* − Hms^- Ybt^-) Lcr^-	25
KIM6-2046.1	Hms^+ Ybt^- (*irp2*::*kan2046.1*) Lcr^- Km^r	25
KIM6-2055	Hms^+ Ybt^- (*ybtA*::*kan2055*) Lcr^- Km^r	23
KIM6-2085+	Hms^+ Ybt^- (Δ*ybtD2085*) Lcr^-	This study
KIM6-2086	Hms^+ Ybt^- (*irp1-2086*) Lcr^-	This study
KIM6-2086.1+	Pgm^+ (Hms^+ Ybt^+) Lcr^-; derived from KIM6-2086 by replacement of the *irp1-2086* mutation with $irp1^+$	This study
Plasmids		
pACYC184	4.2-kb cloning vector; Cm^r Tc^r	17
pEU730	15.2-kb low-copy-number vector with promoterless *lacZ*; Spc^r Sm^r	28
pEUYbtP	15.4-kb low-copy-number *ybtP*::*lacZ* reporter plasmid, Spc^r; iron-, Fur-, and YbtA-regulated expression of β-galactosidase	24
pKNG101	6.8-kb suicide vector; $sacB^+$, R6K origin; Suc^s Sm^r	44
pWSK29	5.4-kb low-copy-number cloning vector; Ap^r	74
pET22b-HMWP1-TEmut	9.49-kb *Nco*I/*Xho*I fragment of *irp1*, with altered bp, in pET22b; Ap^r, 15.0 kb, *irp1-2086* (HMWP1-S2908A)	Z. Suo and C. T. Walsh
pEUYbtD1	15.4-kb low-copy-number *ybtD*::*lacZ* reporter plasmid; 182-bp *Asc*I/*Kpn*I fragment containing *ybtD* promoter region cloned into *Asc*I/*Kpn*I sites of pEU730; Spc^r Sm^r; fusion of *ybtD* 167-bp promoter to *lacZ*	This study
pEUYbtD2	15.6-kb low-copy-number *ybtD*::*lacZ* reporter plasmid; 355-bp *Asc*I/*Kpn*I fragment containing *ybtD* promoter region cloned into *Asc*I/*Kpn*I sites of pEU730; Spc^r Sm^r; fusion of *ybtD* 342-bp promoter to *lacZ*	This study
pIrp1TE2	1.37-kb *Pvu*II/*Xho*I fragment from pET22b-HMWP1-TEmut cloned in *Sma*I/*Sal*I sites of suicide vector pKNG101; Suc^s Sm^r, 8.2 kb, *irp1-2086* (HMWP1-S2908A)	This study
pKNGIRP1	1,703-bp PCR product from pPSN3 ligated into the *BamH*I/*Xba*I site of pKNG101; $sacB^+$, R6K origin; Suc^s Sm^r, 8.5 kb; $irp1\text{-}TE^+$	This study
pPSN3	9,994-bp *Sal*I fragment encompassing the *irp1-ybtE* region in pBLG2; Ap^r; 15.8 kb	24
pYBTD1	4.44-kb *Xho*I/*Bgl*II fragment from *Y. pestis* KIM6+ genomic DNA cloned into *Xho*I/*Bam*HI sites of pWSK29; Ap^r; 9.8 kb; $ybtD^+$	This study
pYBTD2	774-bp *Eco*RV/*Asu*II fragment within *ybtD* removed from pYBTD1; Ap^r; 9.0 kb; Δ*ybtD*	This study
pYBTD3	3.7-kb *Xba*I/*Apa*I fragment from pYBTD2 cloned into *Xba*I/*Apa*I sites of suicide vector pKNG101; Suc Sm^r; Δ*ybtD*	This study
pYBTD4	0.93-kb *Bam*HI/*Xba*I PCR product of *ybtD* and its putative promoter region ligated into *Bam HI*/*Xba*I sites of pACYC184; Cm^r; 10.5 kb; $ybtD^+$	This study

[a] *Y. pestis* strains with a plus sign possess an intact 102-kb *pgm* locus containing the genes for hemin storage (*hms*) and the Ybt system. All other *Y. pestis* strains contain a mutation within the *pgm* locus due to either a deletion or insertion of an antibiotic resistance cassette. Strains synthesizing the siderophore Ybt are designated Ybt^+, while those affected in Ybt production are Ybt^-. Lcr^- indicates the absence of the low-calcium-response virulence plasmid pCD1. Abbreviations: Ap^r, Km^r, Spc^r, Sm^r, Tc^r, and Cm^r, resistance to ampicillin, kanamycin, spectinomycin, streptomycin, tetracycline, and chloramphenicol, respectively.

*Xba*I sites of pKNG101, generating pKNGIRP1. The wild-type sequence was introduced into *Y. pestis* KIM6-2086 by allelic exchange as described previously (5). Allelic exchange was confirmed by sequencing a PCR product from the *irp1-TE* region.

Protein analyses. To label cellular proteins, whole cells of *Y. pestis* strains were grown through two passages in PMH2, with or without 10 μM $FeCl_3$, for a total of approximately six generations and labeled with ^{35}S-amino acids (DuPont NEN Research Products) for 1 h as previously described (26). To analyze the effect of Ybt on protein synthesis, Ybt, in the form of KIM6+ culture supernatant, was added at the same time as ^{35}S-amino acids to cells acclimated to iron starvation. An equivalent number of counts was electrophoresed on 9% polyacrylamide gels containing sodium dodecyl sulfate (SDS). Dried gels were exposed to Kodak BioMax MR film at room temperature.

Ybt bioassay. Culture supernatants were obtained from *Y. pestis* cells inoculated into deferrated PMH2 and grown for a total of six to nine generations at 37°C as previously described (25). Cells were pelleted by centrifugation, and the supernatant was filtered through a 0.2-μm-pore-size filter. For growth responses, PMH-S, PMH2-S, and/or PMH-DIP plates were overlayered with 0.04 optical density (at 620 nm) units of KIM6-2046.1 (*irp2*::kan2046.1) cells grown in deferrated PMH2 and 25 μl of filtered supernatants from iron-deficient cultures was added to wells in the plates.

The Δ*ybtD* and *irp1-2086* mutants were also tested for their ability to promote the growth of KIM6-2046.1 at 37°C by streaking the mutants adjacent to KIM6-2046.1 on PMH-S, PMH2-S, and/or PMH-DIP plates. Prior to streaking, the mutants were adapted to iron-deficient growth conditions as described above. *Y. pestis* strains that do not produce Ybt are unable to grow on PMH-S, PMH2-S, or PMH-DIP at 37°C but can be cross-fed by Ybt-producing strains (33).

Generating *ybtD* promoter fusions with *lacZ*. Two PCR products were amplified from pYBTD1 using ProofStart *Taq* polymerase, digested with *Kpn*I and *Asc*I, and ligated into the *Asc*I/*Kpn*I sites of pEU730. The forward primer for both constructs was EntD.pF (5′-AGGCGCGCCAATAATTGTGAAGTATCA TTTCA-3′). For the 167-bp insert (pEUYbtD1) and the 342-bp insert (pEU-

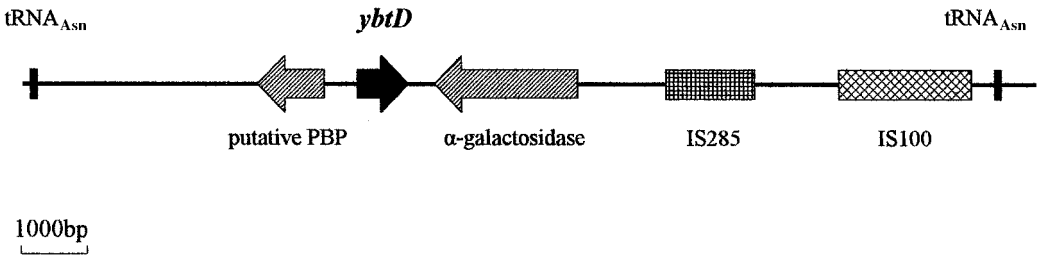

FIG. 1. Region of *Y. pestis* KIM10+ genome containing *ybtD*. The genes encoding two asparaginyl tRNAs, a putative periplasmic binding protein (PBP) for a C4-dicarboxylate ABC transporter, a RafA-like α-galactosidase, and YbtD are indicated as well as IS*285* and IS*100* elements. Arrows indicate the direction of transcription of selected genes.

YbtD2), primers EntD.pR-1 (5′-GGGGTACCGCGTTACCCTAATTATCTTA ATC-3′) and EntD.pR-2 (5′-GGGGTACCGCCTTGTTCAGACTCCCAG-3′) were used, respectively. Reactions for both products consisted of 3 min at 94°C, followed by 25 cycles of 20 s at 94°C, 30 s at 55°C, and 30 s at 72°C and a single cycle at 72°C for 7 min. The cloned promoter regions were sequenced to confirm that no PCR errors had been introduced.

β-Galactosidase assays. Lysates were prepared from cells carrying the *ybtP*::*lacZ* or *ybtD*::*lacZ* reporter plasmid. The cells were grown in PMH2 in the presence or absence of iron through two transfers for a total of approximately six generations, as previously described (69). β-Galactosidase activities were measured spectrophotometrically with a Genesys5 spectrophotometer (Spectronic Instruments, Inc.) following cleavage of ONPG (4-nitro-phenyl-β-D-galactopyranoside). Activities are expressed in Miller units (52).

RESULTS

Mutation of *ybtD* causes a loss of Ybt siderophore production. The initiating step in assembling the siderophore on the NRPS/PKS complex is phosphopantetheinylation of carrier sites on HMWP1 and HMWP2. However, a P-pant transferase is not encoded within the HPI of the yersiniae. A BLAST search of the two *Y. pestis* genomes using the amino acid sequence of *E. coli* EntD identified two strong P-pant transferase candidates. One gene product was highly similar to *E. coli* ACPS (acyl carrier protein synthase; 77% identity and 91.3% similarity over the 126 amino acids of both proteins) and is likely the essential P-pant transferase for fatty acid synthesis (46). The other gene was designated *ybtD* and lies between two $tRNA^{Asn}$ approximately 14.2 kb apart (Fig. 1). The *ybtD* open reading frame has multiple potential start sites encoding proteins ranging from 27.5 to 17.5 kDa (246 to 156 amino acids; Fig. 2). YbtD shows high similarities to *Photorhabdus luminescens* NgrA and *Vibrio cholerae* VibB—both involved in siderophore biosynthesis (18, 76). Figure 3 shows an alignment of YbtD, using the first potential start site, with NgrA, VibB, and EntD, the *E. coli* P-pant transferase required for enterobactin biosynthesis (1, 19, 32). In addition to containing the two conserved domains found in P-pant transferases, (46) these proteins also display strong homology at the N terminus (residues 34 to 112 of YbtD in Fig. 3).

A *ybtD* deletion was constructed and crossed into *Y. pestis* KIM6+ using allelic exchange (see Materials and Methods). PMH-S, PMH2-S, and/or PMH-DIP were used to examine the effect of the mutation on the ability of this strain to grow at 37°C under iron-chelated conditions. KIM6-2085+ (Δ*ybtD2085*) did not grow at 37°C on the iron-chelated media (Table 2), indicating that the mutated strain lost the ability to either synthesize and secrete or utilize Ybt. Supernatants from iron-deficient cultures of KIM6-2085+ were unable to stimulate the growth of a *Y. pestis* strain (KIM6-2046.1) defective in Ybt synthesis (Table 2). However, culture supernatants from KIM6+, a Ybt-producing strain of *Y. pestis*, restored growth of KIM6-2046.1 cells under these conditions. In addition, KIM6+ was able to cross-feed KIM6-2085+ as well as KIM6-2046.1 cells (Table 2). This suggests that the $YbtD^-$ mutant is defective in synthesis of the Ybt siderophore but is still able to use it.

For complementation analyses, a PCR product encompassing the *ybtD* gene was cloned into pACYC184 and designated pYBTD4. The recombinant plasmid restored the ability of KIM6-2085+ cells to grow on iron-chelated plates at 37°C. In addition, culture supernatant from the complemented strain was able to promote the growth of KIM6-2046.1 (*irp2*::*kan2046.1*) on PMH-DIP plates (Table 2).

The Δ*ybtD2085* mutation results in decreased expression of *ybt* operons. Previously we showed that most mutations (e.g., Δ*ybtE*, Δ*ybtU*, Δ*irp2*, and *irp1*::*kan*) which result in the loss of siderophore production lower the expression of other Ybt biosynthetic genes (HMWP1, HMWP2, and YbtE) as well as the Ybt receptor (Psn) (4, 23, 33). However, two mutations in genes encoding Ybt biosynthetic enzymes (Δ*ybtT* and Δ*ybtS*) did not affect the expression of these indicator proteins (33). To determine the effect, if any, of the Δ*ybtD2085* mutation on the expression of these indicator proteins, total ^{35}S-labeled proteins synthesized by cells grown under iron-sufficient and iron-deficient conditions were analyzed by SDS-polyacrylamide gel electrophoreis (PAGE). The protein expression pattern of the $YbtD^-$ mutant was similar to that of the Δ*ybtE*, Δ*ybtU*, Δ*irp2*, and *irp1*::*kan* mutants that are defective in siderophore biosynthesis. In the absence of iron, the level of expression of HMWP1, HMWP2, and Psn proteins was greatly reduced in KIM6-2085+ (Δ*ybtD2085*) cells (Fig. 4, lane 3) compared to that in the parental strain KIM6+ (Fig. 4, lane 1). In this experiment, YbtE was not detected due to inadequate separation of the polypeptides in this size range. The reduced level of Psn expressed in the $YbtD^-$ mutant was similar to that observed in KIM6-2046.1 (Fig. 4, lane 2); HMWP1 and HMWP2 are not detected in KIM6-2046.1 cells because of the *irp2*::*kan2046.1* mutation and its polar effects. Complementation of the $YbtD^-$ mutant with pYBTD4, encoding *ybtD*, restored expression of HMWP1, HMWP2, and Psn (Fig. 4, lane 4). We have previously shown that addition of purified Ybt or supernatant containing Ybt to *Y. pestis* Ybt biosynthetic mu-

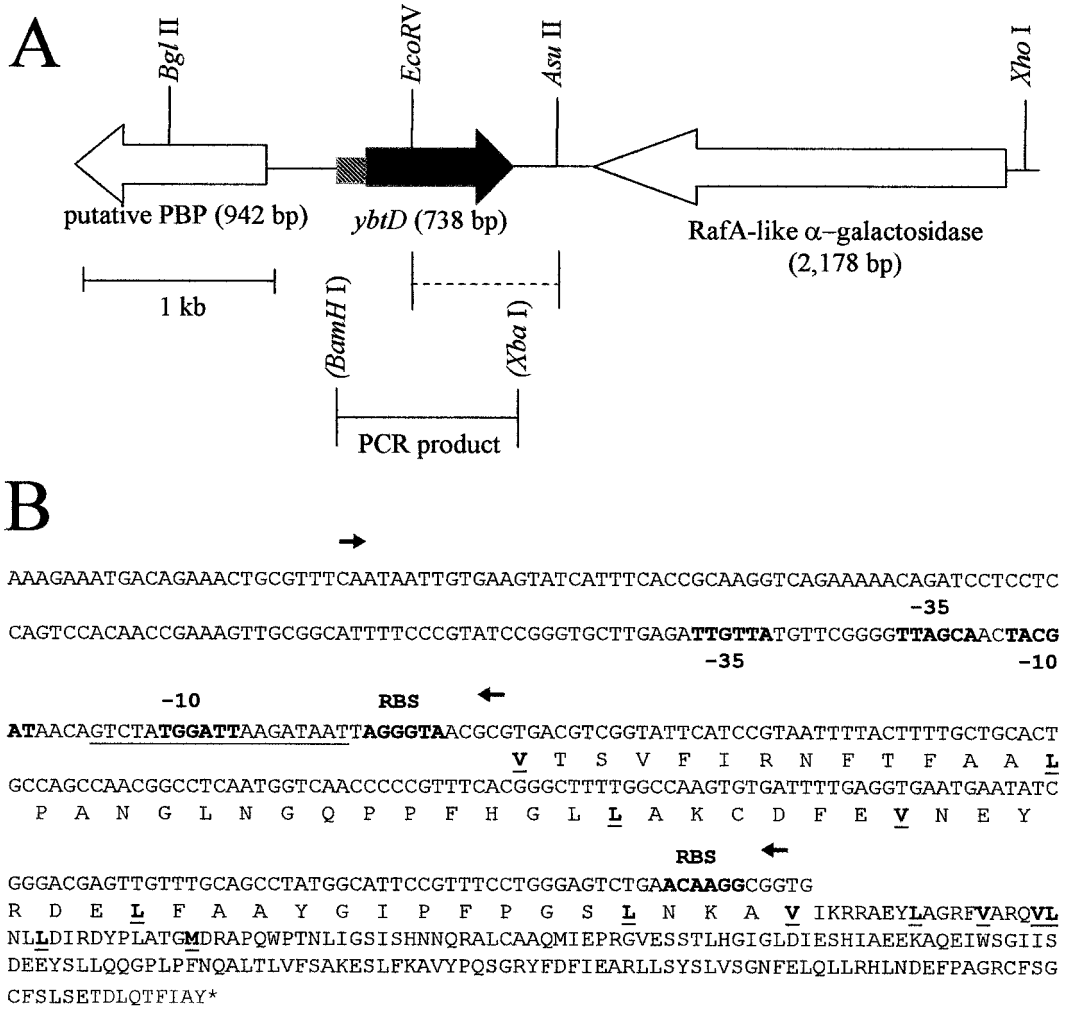

FIG. 2. Genetic organization of the *Y. pestis ybtD* region showing restriction sites used. (A) Dashed line indicates the region deleted in the Δ*ybtD* mutant. The PCR product used in complementation studies is also indicated. The *Bam*HI and *Xba*I sites in parentheses are artificial restriction sites introduced by PCR. (B) Putative −10 and −35 regions, potential ribosomal binding sites (RBS), and a region with similarity to a Fur binding site (underlined nucleotides), as well as the potential protein start sites, are indicated (underlined and in boldface type). Arrows show the two promoter regions tested in expression studies.

tants restores expression of HMWP1, HMWP2, YbtE, and Psn (4, 23, 33, 55). Likewise wild-type levels of HMWP1, HMWP2, and Psn were expressed by iron-deficient cultures of the YbtD$^-$ cells labeled in the presence of supernatant from KIM6+ (expressing Ybt siderophore) but not with supernatant from the Ybt-biosynthetic mutant KIM6-2046.1 (Fig. 4, lanes 5 and 6).

We used pEUYbtP, a *ybtP* promoter fusion to *lacZ*, to test the effect of the *ybtD2085* mutation on gene transcription. Previous studies showed that the *ybtP* promoter is regulated by Fur, iron, YbtA, and the Ybt siderophore (23, 24, 33). Because our *Y. pestis* strains are phenotypically β-galactosidase negative, any β-galactosidase activity is due to the presence of the reporter plasmid (33, 70). The β-galactosidase activities of cells bearing pEUYbtP and grown in deferrated PMH2 in the presence or absence of added iron, are presented in Table 3. As expected, expression of *lacZ* from the *ybtP* promoter was iron regulated in KIM6+, which contains all the genes needed for Ybt synthesis and utilization; there was an 18.4-fold repression of β-galactosidase activity in cells grown in the presence of surplus iron compared to those cultured under iron-deficient conditions. Expression of the *ybtP*::*lacZ* reporter in the YbtD$^-$ mutant, KIM6-2085+, was still somewhat iron regulated (14-fold repression); however, compared to KIM6+, the overall expression was greatly reduced (a 9.8-fold reduction in iron-starved cultures [Table 3]). Similar results were observed with the *ybtP*::*lacZ* reporter in KIM6-2046.1, an HMWP2$^-$ mutant unable to synthesize Ybt (Table 3). As in previous studies (24), *lacZ* expression from pEUYbtP in a Δ*pgm* mutant was even lower, likely due to the absence of the YbtA transcriptional activator (Table 3). These studies suggest that loss of expression of HMWP1, HMWP2, and Psn in the YbtD$^-$ mutant is the result of decreased transcription from the relevant *ybt* promoters.

Transcription of *ybtD* is not affected by YbtA or iron status of the cell. The promoters of other *ybt* genes encoding siderophore biosynthetic and transport functions are repressed by iron through the action of Fur and are activated by YbtA and

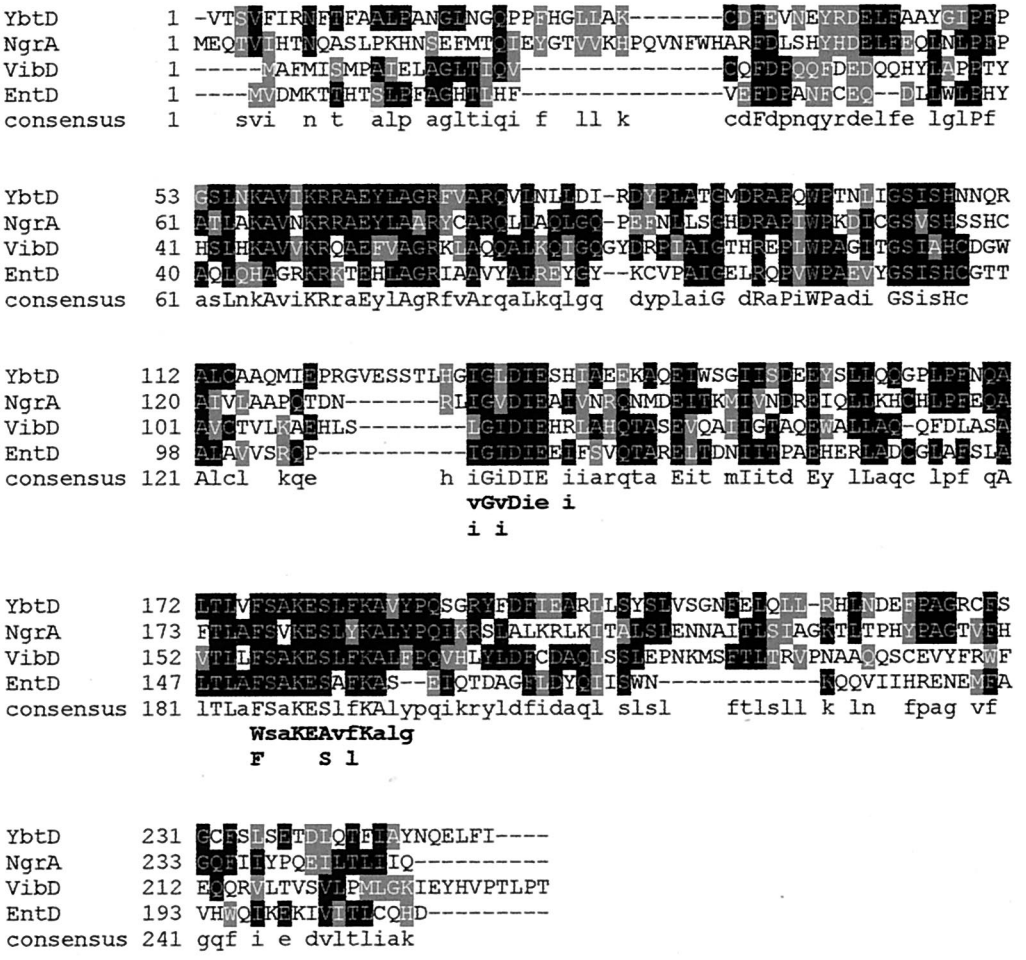

FIG. 3. Amino acid sequence alignment of YbtD from *Y. pestis*, NgrA from *P. luminescens*, VibD from *V. cholerae*, and EntD from *E. coli*. Residues with identity to YbtD are in white with a solid black background. Conservative and semiconservative amino acid substitutions are shaded. The consensus line shows identical residues in all four proteins (uppercase letters) and identical residues in two or more proteins (lowercase letters). The identity and similarity of YbtD to each of these proteins are 34 and 65.3% (NgrA), 31.3 and 60.2% (VibD), and 27.2 and 58.5% (EntD). The residues below the consensus line indicate conserved (lowercase) and highly conserved (uppercase) amino acids within the proposed P-pant transferase domain derived from comparison of 22 P-pant transferases (46).

the siderophore (4, 23, 24, 69). Due to the multiple possible protein start sites and the two potential −10 and −35 regions (Fig. 2B), we constructed two transcriptional reporters to examine expression from the *ybtD* promoter. Both constructs start with the same upstream site (left-pointing arrow in Fig. 2B) and include both −10 and −35 regions and the potential Fur binding site; the 167-bp promoter fragment (pEUYbtD1) ends at the first potential valine start site, while the longer 342-bp construct (pEUYbtD2) ends at the third potential valine start (two right-pointing arrows in Fig. 2B) to ensure that all potential transcriptional regulatory elements were included. These regions were cloned into the *lacZ* transcriptional fusion vector, pEU730 (28), which contains an RNase III site upstream of *lacZ* (29). Processing of the message at this site removes any sequences which might alter message stability or affect translational efficiency (47). The level of β-galactosidase activity from *Y. pestis* KIM6(pEUYbtD2)+ cells grown under iron-sufficient or iron-deficient conditions was ~2-fold lower than that determined in *Y. pestis* KIM6(pEUYbtD1)+ cells (Table 3). Since the amino acid similarities between YbtD and other P-pant transferases start upstream of the third potential valine start, we used pEUYbtD1 to further characterize the *ybtD* promoter region. The *ybtD*::*lacZ* reporter failed to show any repression under iron-sufficient growth conditions (Table 3). In addition, the level of β-galactosidase activity was similar in $YbtA^+$ and $YbtA^-$ strains of *Y. pestis* bearing pEUYbtD1 (Table 3). Thus, the *ybtD* promoter does not appear to be regulated by iron or YbtA.

A single amino acid substitution in the TE domain of HMWP1 causes loss of siderophore production. HMWP1 contains an internal TE domain which is hypothesized to be involved in the final step of siderophore biogenesis: release of the siderophore from the biosynthetic machinery. Previously we showed that YbtT, which contains a TE domain, is required for siderophore synthesis in *Y. pestis* (33) and likely serves an editing function to release aberrant intermediates on carrier sites of HMWP1 and HMWP2. To determine if the internal TE domain in HMWP1 is required for Ybt synthesis, we con-

TABLE 2. Growth of *Y. pestis* KIM6+ and *ybt* mutants on PMH-S, PMH2-S, and/or PMH-DIP

Strain	Relevant characteristic	Growth on PMH-DIP, PMH-S, and/or PMH2-S[a]	Growth stimulation of KIM6-2046.1 on PMH-DIP, PMH-S, and/or PMH2-S[b]	Growth stimulation by KIM6+ on PMH-DIP, PMH-S, and/or PMH2-S[c]
KIM6+	*ybt*$^+$	+	+	ND[d]
KIM6-2046.1	*irp2*::*kan2046.1*	−	−	+
KIM6-2085+	Δ*ybtD20285*	−	−	+
KIM6-2085(pYBTD4)+	Δ*ybtD20285*/*ybtD*$^+$	+	+	ND
KIM6-2086	*irp2-2086*	−	−	+
KIM6-2086.1+	*ybt*$^+$	+	+	ND

[a] The presence or absence of growth on PMH-S, PMH2-S, and PMH-DIP plates at 37°C is denoted as + or −, respectively.
[b] Each strain was tested for its ability to promote the growth of KIM6-2046.1 (*irp2*::*kan2046.1*) at 37°C on PMH-S, PMH2-S, and PMH-DIP plates, either by streaking adjacent to KIM6-2046.1 or by spent culture supernatants.
[c] Strains were tested for their ability to use exogenous Ybt siderophore at 37°C by streaking adjacent to KIM6+ on PMH-S, PMH2-S, and/or PMH-DIP plates or by spent culture supernatants.
[d] ND, not determined.

structed a mutation that results in the substitution of an alanine for the serine at residue 2908 within the catalytic TE domain of HMWP1 (Fig. 5). Mutational analysis of several TEs showed that the conserved serine residue in the G(Y/W/H)SXG motif is a required catalytic nucleophile (67). Allelic exchange was used to introduce this mutation into KIM6+ generating strain KIM6-2086. KIM6-2086 cells were unable to grow on PMH2-S or PMH-DIP plates at 37°C unless supplied with culture supernatant from KIM6+ cells containing the Ybt siderophore. Growth on PMH2-S plates at 37°C was also restored when the chromosomal mutation was replaced by the wild-type sequence (strain KIM6-2086.1+, Table 2). Finally, culture supernatant from iron-starved KIM6-2086 cells did not allow the growth of the Ybt-biosynthetic mutant, KIM6-2046.1, on PMH2-S plates (Table 2). These results indicate that the mutation in the TE domain of *irp1* caused a loss of siderophore production and/or secretion.

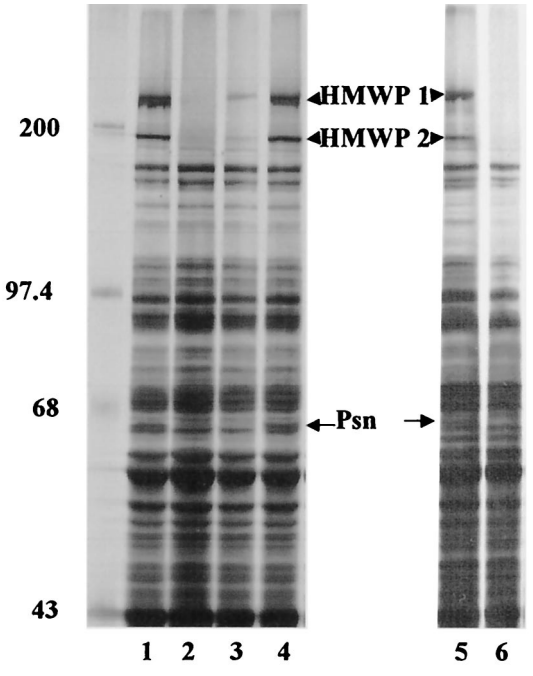

FIG. 4. SDS-PAGE analysis of whole-cell proteins from *Y. pestis* strains grown in iron-deficient PMH2. Cultures from *Y. pestis* KIM6+ (lane 1), KIM6-2046.1 (*irp2*::*kan2046.1*) (lane 2), KIM6-2085+ (Δ*ybtD2085*) (lane 3), and KIM6-2085(pYBTD4)+ (Δ*ybtD2085*/*ybtD*$^+$) (lane 4) were incubated with ^{35}S-labeled amino acids for 1 h. To demonstrate the effect of exogenous siderophore on expression of proteins by KIM6-2085+ cells, KIM6+ culture supernatant containing Ybt siderophore (lane 5) or KIM6-2046.1 culture supernatant (lane 6) was added 1:1 at the same time as ^{35}S-labeled amino acids. Total cellular proteins were separated on a 9% polyacrylamide gel and visualized by autoradiography. Sizes of molecular mass markers (in kilodaltons) are indicated. Arrows point to the iron-regulated proteins HMWP1 (240 kDa), HMWP2 (190 kDa), and Psn (68 kDa).

The *irp1-2086* mutation does not affect the expression of *ybt* operons. To determine whether expression of Ybt proteins was affected by the *irp1-2086* mutation, total ^{35}S-labeled proteins synthesized by cells grown under iron-deficient conditions were analyzed by SDS-PAGE. The protein expression pattern of the HMWP1-TE mutant (KIM6-2086) was similar to that of Ybt$^+$ strain KIM6+; i.e., HMWP1, HMPW2, and Psn were highly expressed in the mutant (Fig. 6). In addition, the β-galactosidase activity of KIM6-2086 cells bearing pEUYbtP and grown in deferrated PMH2 was repressed by iron (16.5-fold repression). The levels of *lacZ* expression were similar to that observed with KIM6+ which produces and uses the Ybt siderophore (Table 3). Thus, the *irp1-2086* mutation did not affect the expression of *ybt* genes.

DISCUSSION

PK synthases, fatty acid synthases, and nonribosomal peptide synthetases all require posttranslational modification of the acyl, aryl, and/or peptidyl carrier protein domains for catalytic activation, the first step in the biogenesis of their products. The last step in this process is release of the product from the enzyme complex by a TE. In this study we have examined the roles of YbtD, a putative P-pant transferase for the Ybt synthetase complex, and the TE domain of HMWP1, which likely releases the completed molecule, in siderophore production.

P-pant transferases activate the enzyme complex by catalyzing transfer of P-pant moieties from coenzyme A molecules to the carrier domains of PK synthases, fatty acid synthases, and nonribosomal peptide synthetases (46). Ybt siderophore is synthesized via a mixed NRPS/PK synthetase mechanism. HMWP1 contains one acyl and one peptidyl carrier domain,

TABLE 3. β-Galactosidase activities of *Y. pestis* strains containing either a *ybtP*::*lacZ* or a *ybtD*::*lacZ* reporter plasmid[a]

Reporter	Strain	Mean β-galactosidase activity[b] (Miller units) ± SD of cells grown:		Ratio (growth without Fe/ growth with Fe)	Ratio (WT/Mutant) for cells grown:	
		Without iron	With iron		Without iron	With iron
pEUYbtP (*ybtP*::*lacZ*)	KIM6+ (*ybt*$^+$)	29,929 ± 1,582	1,626 ± 249	18.4	ND[c]	ND
	KIM6 (Δ*pgm* [*ybt*])	656 ± 142	216 ± 26	3.0	45.6	7.5
	KIM6-2046.1 (*irp2*::*kan2046.1*)	4,351 ± 1,705	292 ± 20	14.9	6.9	5.6
	KIM6-2085+ (Δ*ybtD2085*)	3,044 ± 249	218 ± 17	14.0	9.8	7.5
	KIM6-2086 (*irp1-2086*)	34,004 ± 4,963	2,058 ± 580	16.5	0.88	0.79
pEUYbtD1 (*ybtD*::*lacZ*; 167-bp promoter region	KIM6+ (*ybt*$^+$)	4,252 ± 1,415	4,674 ± 1,236	0.91	ND	ND
	KIM6-2055 (*ybtA*::*kan2055*)	4,811 ± 982	ND	ND	0.88	ND
pEUYbtD2 (*ybtD*::*lacZ*; 342-bp promoter region	KIM6+ (*ybt*$^+$)	2,637 ± 446	2,072 ± 307	1.3	ND	ND

[a] Cells were harvested during exponential growth at 37°C after approximately six generations in PMH2 containing either no added iron or 10 μM $FeCl_3$.
[b] Enzyme activities are expressed in Miller units (52). The values ± standard deviations represent an average of three to four individual reactions from two or more independent cultures.
[c] ND, not determined or not applicable.

while HMWP2 possesses an aryl and two peptidyl carrier domains (30). While there are some differences among the HPIs of the pathogenic yersiniae, all encode an essentially identical and interchangeable siderophore biosynthesis and transport system and none of the pathogenicity islands possess a gene encoding the essential P-pant transferase activity (12, 24, 25, 30, 54, 55, 60).

The HPI of *Y. pseudotuberculosis* can insert at any one of three different $tRNA^{Asn}$ genes; only one HPI insertion site has been identified in three different strains of *Y. pestis* (10, 30, 38, 53). The region of KIM10+ chromosomal DNA that contains *ybtD* is flanked by two $tRNA^{Asn}$ genes (Fig. 1). Sequences adjacent to the *Y. pseudotuberculosis* and *Y. enterocolitica* HPIs (3, 10, 38, 60) are homologous to the sequences flanking these tRNA genes. Thus, it is possible that in some strains of *Y. pseudotuberculosis* and *Y. enterocolitica* the HPI is located close to the region containing *ybtD*. In KIM10+, the two $tRNA^{Asn}$ in the vicinity of *ybtD* are approximately 14.2 kb apart (Fig. 1). However, in CO92, these same two tRNA genes are separated by >179 kb. (53) This difference between KIM10+ and CO92 probably results from an inversion involving the IS*285* element (Fig. 1).

We have demonstrated that *ybtD* is essential for normal production of the Ybt siderophore. Although the authentic start site for YbtD remains to be determined, this protein contains two conserved P-pant transferase domains (Fig. 3), suggesting that it is required to activate the carrier domains of

```
Consensus GxSxG-22-24aa - D-~100 aa-gxH
YbtT      GHSMG - 46 aa - D - 80 aa-GDH
HMWP1-TE  GWSYG - 23 aa - D -121 aa-ASH
```

FIG. 5. Conserved TE domains of YbtT and HMWP2. The TE consensus sequence is described in reference 67. The serine residue in HMWP1 that was changed to an alanine in KIM6-2086 is underlined.

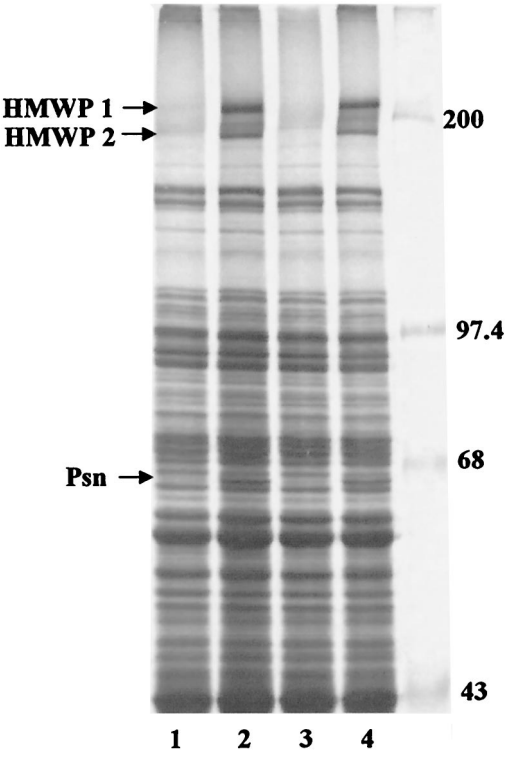

FIG. 6. SDS-PAGE analysis of whole-cell proteins from *Y. pestis* strains grown in iron-sufficient and iron-deficient PMH2. Cultures from *Y. pestis* KIM6+ (lanes 1 and 2), KIM6-2046.1 (*irp2*::*kan2046.1*) (lane 3), and KIM6-2086 (*irp1-2086*) (lane 4) were incubated with ^{35}S-labeled amino acids for 1 h. Total cellular proteins were separated on a 9% polyacrylamide gel and visualized by autoradiography. Cell extracts from iron-deficient cultures (lanes 2 to 4) or iron-sufficient cultures (lane 1) are shown. Sizes of molecular mass markers (in kilodaltons) are indicated. Arrows point to the iron-regulated proteins HMWP1 (240 kDa), HMWP2 (190 kDa), and Psn (68 kDa).

HMWP1 and HMWP2. Bioassays using the Δ*ybtD* mutant indicate that it is defective in Ybt siderophore production (Table 2). Our bioassay detects Ybt in iron-deficient culture supernatants diluted 1:16 (data not shown). Thus, if any Ybt siderophore is present in culture supernatants of the YbtD$^-$ mutant it is present at <6% of wild-type levels.

Surprisingly, transcription from the *ybtD* promoter is not regulated by the iron status of the cell or by YbtA (Table 3). This suggests that *ybtD* may have been recently converted for use in the Ybt system or that this P-pant transferase is used to activate more than one system. The *Y. pestis* KIM10+ (21) and CO92 genomes (53) both contain two NRPS systems in addition to Ybt that would require activation by a P-pant transferase. One system encodes enzymes with homologies to *Bordetella* siderophore biosynthetic enzymes as well as an OM receptor and an ABC transporter related to similar components in other iron transport systems (34, 43, 56). The second putative NRPS system contains open reading frames showing similarities to *Yersinia* HMWP1 and HMWP2 proteins and to YbtP, a fused function permease/ATP hydrolase ABC transporter component. To be functional, both these systems would require activation by a P-pant transferase, possibly YbtD. It is unlikely that the *Y. pestis* ACPS would work since in *E. coli*, the ACPS P-pant transferase activity is specific for fatty acid biosynthesis (46). However, it is unknown whether either of these putative NRPS systems is functional.

The Ybt system, like many bacterial NRPS and/or PK synthase systems, possesses a C-terminal TE domain as part of the NRPS/PK synthetase enzyme (HMWP1) in addition to a separate gene encoding an external TE (YbtT). We have now shown that both YbtT (33) and the HMWP1-TE domain (this study) are required for normal levels of Ybt siderophore production. Thus, these putative TEs do not perform redundant functions but are apparently required in separate aspects of Ybt biogenesis. It has previously been proposed that an internal TE domain likely releases the completed molecule from the enzyme complex while an external TE may serve an editing function by removing aberrant structures on mischarged NRPSs caused by nonspecific thioesterification (13, 49, 65).

In *Y. pestis*, we proposed that Ybt (or the Ybt-Fe complex) functions as a signal molecule in concert with the AraC-type regulator YbtA to activate transcription of other genes in the Ybt system and repress transcription of *ybtA*. Thus, YbtA$^-$ mutants showed reduced β-galactosidase activity from *psn*::*lacZ* and *ybtP*::*lacZ* reporter plasmids but elevated expression from a *ybtA*::*lacZ* reporter. An *irp2*::*kan2046.1* mutation also lowered expression of the *psn* and *ybtP* promoters but to a lesser extent than the *ybtA*::*kan2055* mutation (23, 24) (Table 3). This suggests that YbtA alone may partially activate promoters controlled by this regulator (23). In addition, strains with large deletions or insertions in *irp1*, *irp2*, *ybtE*, or *ybtD* genes, encoding products involved in Ybt synthesis, had significantly reduced expression of HMWP1, HMWP2, as well as Psn (25) (Fig. 4 and 6). In contrast, mutations in *ybtT* or *ybtS* and now in the TE domain of *irp1* eliminate siderophore synthesis without affecting *ybt* gene expression (33) (Fig. 6). These results bring into question the role of Ybt in regulating expression of the *ybt* operons. However, it is possible that both the HMWP1-TE$^-$ and YbtT$^-$ mutants produce amounts of Ybt siderophore sufficient for regulatory activity but below our level of detection (~6% of wild-type levels) in bioassays. If YbtT serves a proofreading function and removes aberrant structures from the enzyme complex, low levels of authentic Ybt might be produced in vivo in this mutant. Indeed, YbtT is not required for in vitro synthesis of Ybt using purified compounds (51). Alternatively, YbtT$^-$ mutants may produce an aberrant compound(s) that can function as an inducer in concert with YbtA yet not be effective in iron transport. The TE domain of HMWP1 likely releases the completed siderophore from the enzyme complex; noncatalytic hydrolysis of the thioester bond could release low levels of Ybt sufficient to fulfill regulatory functions without providing observable growth stimulation. Finally, YbtS is hypothesized to synthesize salicylate, which is activated by YbtE, transferred to the N-terminal aryl carrier protein domain of HMWP2, and initiates Ybt synthesis (30). Albeit at a much lower efficiency, YbtE also adenylates 2,3-dihydroxybenzoate (31). Thus, in the YbtS$^-$ mutant, YbtE may activate 2,3-dihydroxybenzoate or another phenolate compound which then initiates synthesis of an aberrant Ybt molecule. The low efficiency of YbtE-catalyzed activation of an alternate phenolate moiety or poor chain elongation from this aberrant structure may lead to low levels of an altered siderophore that interacts with YbtA and allows normal regulation of the Ybt system. Further experiments will be necessary to completely characterize this regulatory system and to determine the nature of the signal molecule in Ybt$^+$ cells as well as in YbtT$^-$, YbtS$^-$, and HMWP1-TE$^-$ mutants.

ACKNOWLEDGMENTS

This work was supported by Public Health Service grants AI42738 and AI33481 from the National Institutes of Health.

We thank Jennifer Abney for assistance with some of the β-galactosidase assays. We thank Christopher Walsh and Zucai Suo for providing pET22b-HMWP1-TEmut.

REFERENCES

1. **Armstrong, S. K., G. S. Pettis, L. J. Forrester, and M. A. McIntosh.** 1989. The *Escherichia coli* enterobactin biosynthesis gene, entD: nucleotide sequence and membrane localization of its protein product. Mol. Microbiol. **3:**757–766.
2. **Ausubel, F. M., R. Brent, R. E. Kingston, D. D. Moore, J. G. Seidman, J. A. Smith, and K. Struhl (ed.).** 1987. Current protocols in molecular biology. John Wiley & Sons, New York, N.Y.
3. **Bach, S., C. Buchrieser, M. Prentice, A. Guiyoule, T. Msadek, and E. Carniel.** 1999. The high-pathogenicity island of *Yersinia enterocolitica* Ye8081 undergoes low-frequency deletion but not precise excision, suggesting recent stabilization in the genome. Infect. Immun. **67:**5091–5099.
4. **Bearden, S. W., J. D. Fetherston, and R. D. Perry.** 1997. Genetic organization of the yersiniabactin biosynthetic region and construction of avirulent mutants in *Yersinia pestis*. Infect. Immun. **65:**1659–1668.
5. **Bearden, S. W., and R. D. Perry.** 1999. The Yfe system of *Yersinia pestis* transports iron and manganese and is required for full virulence of plague. Mol. Microbiol. **32:**403–414.
6. **Bearden, S. W., T. M. Staggs, and R. D. Perry.** 1998. An ABC transporter system of *Yersinia pestis* allows utilization of chelated iron by *Escherichia coli* SAB11. J. Bacteriol. **180:**1135–1147.
7. **Birnboim, H. C., and J. Doly.** 1979. A rapid alkaline extraction procedure for screening recombinant plasmid DNA. Nucleic Acids Res. **7:**1513–1523.
8. **Braun, V., K. Hantke, and W. Köster.** 1998. Bacterial iron transport: mechanisms, genetics, and regulation, p. 67–145. *In* A. Sigel and H. Sigel (ed.), Metal ions in biological systems, vol. 35. Iron transport and storage in microorganisms, plants, and animals. Marcel Dekker, Inc., New York, N.Y.
9. **Brem, D., C. Pelludat, A. Rakin, C. A. Jacobi, and J. Heesemann.** 2001. Functional analysis of yersiniabactin transport genes of *Yersinia enterocolitica*. Microbiology **147:**1115–1127.
10. **Buchrieser, C., R. Brosch, S. Bach, A. Guiyoule, and E. Carniel.** 1998. The high-pathogenicity island of *Yersinia pseudotuberculosis* can be inserted into any of the three chromosomal *asn* tRNA genes. Mol. Microbiol. **30:**965–978.
11. **Buchrieser, C., M. Prentice, and E. Carniel.** 1998. The 102-kilobase unstable region of *Yersinia pestis* comprises a high-pathogenicity island linked to a

pigmentation segment which undergoes internal rearrangement. J. Bacteriol. **180:**2321–2329.
12. **Buchrieser, C., C. Rusniok, L. Frangeul, E. Couve, A. Billault, F. Kunst, E. Carniel, and P. Glaser.** 1999. The 102-kilobase *pgm* locus of *Yersinia pestis*: sequence analysis and comparison of selected regions among different *Yersinia pestis* and *Yersinia pseudotuberculosis* strains. Infect. Immun. **67:**4851–4861.
13. **Butler, A. R., N. Bate, and E. Cundliffe.** 1999. Impact of thioesterase activity on tylosin biosynthesis in *Streptomyces fradiae*. Chem. Biol. **6:**287–292.
14. **Byers, B. R., and E. L. Arceneaux.** 1998. Microbial iron transport: iron acquisition by pathogenic microorganisms, p. 37–66. *In* A. Sigel and H. Sigel (ed.), Metal ions in biological systems, vol. 35. Iron transport and storage in microorganisms, plants, and animals. Marcel Dekker, Inc., New York.
15. **Carniel, E., I. Guilvout, and M. Prentice.** 1996. Characterization of a large chromosomal "high-pathogenicity island" in biotype 1B *Yersinia enterocolitica*. J. Bacteriol. **178:**6743–6751.
16. **Chambers, C. E., D. D. McIntyre, M. Mouck, and P. A. Sokol.** 1996. Physical and structural characterization of yersiniophore, a siderophore produced by clinical isolates of *Yersinia enterocolitica*. BioMetals **9:**157–167.
17. **Chang, A. C. Y., and S. N. Cohen.** 1978. Construction and characterization of amplifiable multicopy DNA cloning vehicles derived from the P15A cryptic miniplasmid. J. Bacteriol. **134:**1141–1156.
18. **Ciche, T. A., S. B. Bintrim, A. R. Horswill, and J. C. Ensign.** 2001. A phosphopantetheinyl transferase homolog is essential for *Photorhabdus luminescens* to support growth and reproduction of the entomopathogenic nematode *Heterorhabditis bacteriophora*. J. Bacteriol. **183:**3117–3126.
19. **Coderre, P. E., and C. F. Earhart.** 1989. The *entD* gene of the *Escherichia coli* K12 enterobactin gene cluster. J. Gen. Microbiol. **135:**3043–3055.
20. **Cox, C. D., K. L. Rinehart, Jr., M. L. Moore, and C. J. Cook, Jr.** 1981. Pyochelin: novel structure of an iron-chelating growth promoter for *Pseudomonas aeruginosa*. Proc. Natl. Acad. Sci. USA **78:**4256–4260.
21. **Deng, W., V. Burland, G. Plunkett III, A. Boutin, G. F. Mayhew, P. Liss, N. T. Perna, D. J. Rose, B. Mau, S. Zhou, D. C. Schwartz, J. D. Fetherston, L. E. Lindler, R. R. Brubaker, G. V. Plano, S. C. Straley, K. A. McDonough, M. L. Nilles, J. S. Matson, F. R. Blattner, and R. D. Perry.** Genome sequence of *Yersinia pestis* KIM. J. Bacteriol., in press.
22. **Drechsel, H., H. Stephan, R. Lotz, H. Haag, H. Zähner, K. Hantke, and G. Jung.** 1995. Structure elucidation of yersiniabactin, a siderophore from highly virulent *Yersinia* strains. Liebigs Ann. **1995:**1727–1733.
23. **Fetherston, J. D., S. W. Bearden, and R. D. Perry.** 1996. YbtA, an AraC-type regulator of the *Yersinia pestis* pesticin/yersiniabactin receptor. Mol. Microbiol. **22:**315–325.
24. **Fetherston, J. D., V. J. Bertolino, and R. D. Perry.** 1999. YbtP and YbtQ: two ABC transporters required for iron uptake in *Yersinia pestis*. Mol. Microbiol. **32:**289–299.
25. **Fetherston, J. D., J. W. Lillard, Jr., and R. D. Perry.** 1995. Analysis of the pesticin receptor from *Yersinia pestis*: role in iron-deficient growth and possible regulation by its siderophore. J. Bacteriol. **177:**1824–1833.
26. **Fetherston, J. D., and R. D. Perry.** 1994. The pigmentation locus of *Yersinia pestis* KIM6+ is flanked by an insertion sequence and includes the structural genes for pesticin sensitivity and HMWP2. Mol. Microbiol. **13:**697–708.
27. **Fetherston, J. D., P. Schuetze, and R. D. Perry.** 1992. Loss of the pigmentation phenotype in *Yersinia pestis* is due to the spontaneous deletion of 102 kb of chromosomal DNA which is flanked by a repetitive element. Mol. Microbiol. **6:**2693–2704.
28. **Froehlich, B., L. Husmann, J. Caron, and J. R. Scott.** 1994. Regulation of *rns*, a positive regulatory factor for pili of enterotoxigenic *Escherichia coli*. J. Bacteriol. **176:**5385–5392.
29. **Froehlich, B. J., and J. R. Scott.** 1991. A single-copy promoter-cloning vector for use in *Escherichia coli*. Gene **108:**99–101.
30. **Gehring, A. M., E. DeMoll, J. D. Fetherston, I. Mori, G. F. Mayhew, F. R. Blattner, C. T. Walsh, and R. D. Perry.** 1998. Iron acquisition in plague: modular logic in enzymatic biogenesis of yersiniabactin by *Yersinia pestis*. Chem. Biol. **5:**573–586.
31. **Gehring, A. M., I. Mori, R. D. Perry, and C. T. Walsh.** 1998. The nonribosomal peptide synthetase HMWP2 forms a thiazoline ring during biogenesis of yersiniabactin, an iron-chelating virulence factor of *Yersinia pestis*. Biochemistry **37:**11637–11650.
32. **Gehring, A. M., I. Mori, and C. T. Walsh.** 1998. Reconstitution and characterization of the *Escherichia coli* enterobactin synthetase from EntB, EntE, and EntF. Biochemistry **37:**2648–2659.
33. **Geoffroy, V. A., J. D. Fetherston, and R. D. Perry.** 2000. *Yersinia pestis* YbtU and YbtT are involved in synthesis of the siderophore yersiniabactin but have different effects on regulation. Infect. Immun. **68:**4452–4461.
34. **Giardina, P. C., L. A. Foster, S. I. Toth, B. A. Roe, and D. W. Dyer.** 1997. Analysis of the *alcABC* operon encoding alcaligin biosynthesis enzymes in *Bordetella bronchiseptica*. Gene **194:**19–24.
35. **Gong, S., S. W. Bearden, V. A. Geoffroy, J. D. Fetherston, and R. D. Perry.** 2001. Characterization of the *Yersinia pestis* Yfu ABC iron transport system. Infect. Immun. **67:**2829–2837.
36. **Guilvout, I., O. Mercereau-Puijalon, S. Bonnefoy, A. P. Pugsley, and E. Carniel.** 1993. High-molecular-weight protein 2 of *Yersinia enterocolitica* is homologous to AngR of *Vibrio anguillarum* and belongs to a family of proteins involved in nonribosomal peptide synthesis. J. Bacteriol. **175:**5488–5504.
37. **Hare, J. M., and K. A. McDonough.** 1999. High-frequency RecA-dependent and -independent mechanisms of Congo red binding mutations in *Yersinia pestis*. J. Bacteriol. **181:**4896–4904.
38. **Hare, J. M., A. K. Wagner, and K. A. McDonough.** 1999. Independent acquisition and insertion into different chromosomal locations of the same pathogenicity island in *Yersinia pestis* and *Yersinia pseudotuberculosis*. Mol. Microbiol. **31:**291–303.
39. **Heesemann, J., K. Hantke, T. Vocke, E. Saken, A. Rakin, I. Stojiljkovic, and R. Berner.** 1993. Virulence of *Yersinia enterocolitica* is closely associated with siderophore production, expression of an iron-repressible outer membrane polypeptide of 65 000 Da and pesticin sensitivity. Mol. Microbiol. **8:**397–408.
40. **Hornung, J. M., H. A. Jones, and R. D. Perry.** 1996. The *hmu* locus of *Yersinia pestis* is essential for utilization of free haemin and haem-protein complexes as iron sources. Mol. Microbiol. **20:**725–739.
41. **Humphreys, G. O., G. A. Willshaw, and E. S. Anderson.** 1975. A simple method for the preparation of large quantities of pure plasmid DNA. Biochim. Biophys. Acta **383:**457–463.
42. **Jalal, M. A. F., M. B. Hossain, D. van der Helm, J. Sanders-Loehr, L. A. Actis, and J. H. Crosa.** 1989. Structure of anguibactin, a unique plasmid-related bacterial siderophore from the fish pathogen *Vibrio anguillarum*. J. Am. Chem. Soc. **111:**292–296.
43. **Kang, H. Y., T. J. Brickman, F. C. Beaumont, and S. K. Armstrong.** 1996. Identification and characterization of iron-regulated *Bordetella pertussis* alcaligin siderophore biosynthesis genes. J. Bacteriol. **178:**4877–4884.
44. **Kaniga, K., I. Delor, and G. R. Cornelis.** 1991. A wide-host-range suicide vector for improving reverse genetics in Gram-negative bacteria: inactivation of the *blaA* gene of *Yersinia enterocolitica*. Gene **109:**137–141.
45. **Kutyrev, V. V., A. A. Filippov, O. S. Oparina, and O. A. Protsenko.** 1992. Analysis of *Yersinia pestis* chromosomal determinants Pgm^+ and Pst^s associated with virulence. Microb. Pathog. **12:**177–186.
46. **Lambalot, R. H., A. M. Gehring, R. S. Flugel, P. Zuber, M. LaCelle, M. A. Marahiel, R. Reid, C. Khosla, and C. T. Walsh.** 1996. A new enzyme superfamily: the phosphopantetheinyl transferases. Chem. Biol. **3:**923–936.
47. **Linn, T., and R. St. Pierre.** 1990. Improved vector system for constructing transcriptional fusions that ensures independent translation of *lacZ*. J. Bacteriol. **172:**1077–1084.
48. **Lucier, T. S., and R. R. Brubaker.** 1992. Determination of genome size, macrorestriction pattern polymorphism, and nonpigmentation-specific deletion in *Yersinia pestis* by pulsed-field gel electrophoresis. J. Bacteriol. **174:**2078–2086.
49. **Marahiel, M. A., T. Stachelhaus, and H. D. Mootz.** 1997. Modular peptide synthetases involved in nonribosomal peptide synthesis. Chem. Rev. **97:**2651–2673.
50. **Mietzner, T. A., and S. A. Morse.** 1994. The role of iron-binding proteins in the survival of pathogenic bacteria. Annu. Rev. Nutr. **14:**471–493.
51. **Miller, D. A., L. Luo, N. Hillson, T. A. Keating, and C. T. Walsh.** 2002. Yersiniabactin synthetase: a four protein assembly line producing the nonribosomal peptide/polyketide hybrid siderophore of *Yersinia pestis*. Chem. Biol. **9:**333–344.
52. **Miller, J. H.** 1992. A short course in bacterial genetics. A laboratory manual and handbook for *Escherichia coli* and related bacteria. Cold Spring Harbor Laboratory Press, Cold Spring Harbor, N.Y.
53. **Parkhill, J., B. W. Wren, N. R. Thomson, R. W. Titball, M. T. Holden, M. B. Prentice, M. Sebaihia, K. D. James, C. Churcher, K. L. Mungall, S. Baker, D. Basham, S. D. Bentley, K. Brooks, A. M. Cerdeno-Tarraga, T. Chillingworth, A. Cronin, R. M. Davies, P. Davis, G. Dougan, T. Feltwell, N. Hamlin, S. Holroyd, K. Jagels, A. V. Karlyshev, S. Leather, S. Moule, P. C. Oyston, M. Quail, K. Rutherford, M. Simmonds, J. Skelton, K. Stevens, S. Whitehead, and B. G. Barrell.** 2001. Genome sequence of *Yersinia pestis*, the causative agent of plague. Nature **413:**523–527.
54. **Pelludat, C., A. Rakin, C. A. Jacobi, S. Schubert, and J. Heesemann.** 1998. The yersiniabactin biosynthetic gene cluster of *Yersinia enterocolitica*: organization and siderophore-dependent regulation. J. Bacteriol. **180:**538–546.
55. **Perry, R. D., P. B. Balbo, H. A. Jones, J. D. Fetherston, and E. DeMoll.** 1999. Yersiniabactin from *Yersinia pestis*: biochemical characterization of the siderophore and its role in iron transport and regulation. Microbiology **145:**1181–1190.
56. **Perry, R. D., S. W. Bearden, and J. D. Fetherston.** 2001. Iron and heme acquisition and storage systems of *Yersinia pestis*. Recent Res. Dev. Microbiol. **5:**13–27.
57. **Perry, R. D., and J. D. Fetherston.** 1997. *Yersinia pestis*: etiologic agent of plague. Clin. Microbiol. Rev. **10:**35–66.
58. **Perry, R. D., M. L. Pendrak, and P. Schuetze.** 1990. Identification and cloning of a hemin storage locus involved in the pigmentation phenotype of *Yersinia pestis*. J. Bacteriol. **172:**5929–5937.
59. **Perry, R. D., S. C. Straley, J. D. Fetherston, D. J. Rose, J. Gregor, and F. R. Blattner.** 1998. DNA sequencing and analysis of the low-Ca^{2+}-response plasmid pCD1 of *Yersinia pestis* KIM5. Infect. Immun. **66:**4611–4623.
60. **Rakin, A., C. Noelting, S. Schubert, and J. Heesemann.** 1999. Common and

specific characteristics of the high-pathogenicity island of *Yersinia enterocolitica*. Infect. Immun. **67:**5265–5274.
61. **Rakin, A., E. Saken, D. Harmsen, and J. Heesemann.** 1994. The pesticin receptor of *Yersinia enterocolitica*: a novel virulence factor with dual function. Mol. Microbiol. **13:**253–263.
62. **Rossi, M.-S., J. D. Fetherston, S. Létoffé, E. Carniel, R. D. Perry, and J.-M. Ghigo.** 2001. Identification and characterization of the hemophore-dependent heme acquisition system of *Yersinia pestis*. Infect. Immun. **69:**6707–6717.
63. **Sambrook, J., E. F. Fritsch, and T. Maniatis.** 1989. Molecular cloning: a laboratory manual, 2nd ed. Cold Spring Harbor Laboratory Press, Cold Spring Harbor, N.Y.
64. **Sanger, F., S. Nicklen, and A. R. Coulson.** 1977. DNA sequencing with chain-terminating inhibitors. Proc. Natl. Acad. Sci. USA **74:**5463–5467.
65. **Schneider, A., and M. A. Marahiel.** 1998. Genetic evidence for a role of thioesterase domains, integrated in or associated with peptide synthetases, in non-ribosomal peptide biosynthesis in *Bacillus subtilis*. Arch. Microbiol. **169:** 404–410.
66. **Schubert, S., A. Rakin, H. Karch, E. Carniel, and J. Heesemann.** 1998. Prevalence of the "high-pathogenicity island" of *Yersinia* species among *Escherichia coli* strains that are pathogenic to humans. Infect. Immun. **66:** 480–485.
67. **Shaw-Reid, C., N. Kelleher, H. C. Losey, A. M. Gehring, C. Berg, and C. T. Walsh.** 1999. Assembly line enzymology by multimodular nonribosomal peptide synthetases: the thioesterase domain of *Escherichia coli* EntF catalyzes both elongation and cyclolactonization. Chem. Biol. **6:**385–400.
68. **Sikkema, D. J., and R. R. Brubaker.** 1987. Resistance to pesticin, storage of iron, and invasion of HeLa cells by yersiniae. Infect. Immun. **55:**572–578.
69. **Staggs, T. M., J. D. Fetherston, and R. D. Perry.** 1994. Pleiotropic effects of a *Yersinia pestis fur* mutation. J. Bacteriol. **176:**7614–7624.
70. **Staggs, T. M., and R. D. Perry.** 1991. Identification and cloning of a *fur* regulatory gene in *Yersinia pestis*. J. Bacteriol. **173:**417–425.
71. **Suo, Z., C. T. Walsh, and D. A. Miller.** 1999. Tandem heterocyclization activity of the multidomain 230 kDa HMWP2 subunit of *Yersinia pestis* yersiniabactin synthetase: interaction of the 1–1382 and 1383–2035 fragments. Biochemistry **38:**14023–14035.
72. **Surgalla, M. J., and E. D. Beesley.** 1969. Congo red-agar plating medium for detecting pigmentation in *Pasteurella pestis*. Appl. Microbiol. **18:**834–837.
73. **Thompson, J. M., H. A. Jones, and R. D. Perry.** 1999. Molecular characterization of the hemin uptake locus (*hmu*) from *Yersinia pestis* and analysis of *hmu* mutants for hemin and hemoprotein utilization. Infect. Immun. **67:** 3879–3892.
74. **Wang, R. F., and S. R. Kushner.** 1991. Construction of versatile low-copy-number vectors for cloning, sequencing and gene expression in *Escherichia coli*. Gene **100:**195–199.
75. **Weinberg, E. D., and G. A. Weinberg.** 1995. The role of iron in infection. Curr. Opin. Infect. Dis. **8:**164–169.
76. **Wyckoff, E. E., J. A. Stoebner, K. E. Reed, and S. M. Payne.** 1997. Cloning of a *Vibrio cholerae* vibriobactin gene cluster: identification of genes required for early steps in siderophore biosynthesis. J. Bacteriol. **179:**7055–7062.

Editor: J. T. Barbieri